Simulation of Wave Breaking in One-Dimensional Spectral Environment

DMITRY CHALIKOV

Swinburne University of Technology, Victoria, Melbourne, Australia, and P.P. Shirshov Institute of Oceanology, Saint Petersburg, Russia

ALEXANDER V. BABANIN

Swinburne University of Technology, Melbourne, Victoria, Australia

(Manuscript received 21 July 2011, in final form 15 April 2012)

ABSTRACT

Results of numerical investigations, based on full dynamic equations, are presented for wave breaking in a one-dimensional environment with a wave spectrum. The breaking is defined as a process of irreversible collapse of an individual wave in physical space, and the incipient breaker is a wave that reached a dynamic condition of the limiting stability where the collapse has not started yet but is inevitable. The main attention is paid to documenting the evolution of different wave characteristics before the breaking commences. It is shown that the breaking is a localized process that rapidly develops in space and time. No single characteristic, such as wave steepness, wave height, and asymmetry, can serve as a predictor of the incipient breaking. The process of breaking is intermittent; it happens spontaneously and is individually unpredictable. The evolution of geometric, kinematic, and dynamic characteristics of the breaking wave describes the process of breaking itself rather than indicating an imminent breaking. It is shown that the criterion of breaking, valid for the breaking due to modulation instability in one-dimensional waves trains, is not universal if applied to the conditions of spectral environment. In this context, the development of algorithms for parameterization of breaking for wave prediction models and for direct wave simulations is more important.

1. Introduction

Wave breaking is important across a great variety of geophysical, practical, and engineering applications. In the geophysical system of air–sea interactions, the breaking controls the whitecapping dissipation of surface waves and thus the wave growth (e.g., Cavaleri et al. 2007); negotiates the drag coefficient in the atmospheric boundary layer and therefore the momentum and energy fluxes from the wind to the waves; produces turbulence for the upper-ocean mixing (e.g., Chalikov and Belevich 1993); and determines to a great extent the gas, heat, and moisture exchanges across the interface (e.g., Bortkovskii 1987). In hydroacoustics, it is a primary source of the underwater sound (Kerman 1992); in remote sensing, it produces sea spikes (e.g., Melville et al. 1988) and whitecapping, which then serve either as a proxy of wanted properties or an unwanted noise, which needs to be dealt with (e.g., Sharkov 2007). In engineering, it is responsible for impacts on structures and vessels and may directly affect the bottom boundary layer in shallow areas or limit the maximum in probability distributions of wave height, among many other contributions and influences (for a review, see, e.g., Babanin 2011).

For many years, the breaking was regarded as a poorly understood phenomenon that is hard if not impossible to approach by theoretical, numerical, and even experimental means. Indeed, it is a strongly nonlinear process where a wave (or rather wave group, which includes a breaking wave) suddenly, within a fraction of wave period, loses the energy accumulated from the wind over hundreds of wave periods. These events are sporadic (i.e., do not cover the entire wavy surface), and this is in the wave system where all the other processes responsible for the wave evolution are continuous. There are

Corresponding author address: Dmitry Chalikov, Institute of Oceanography Russian Academy of Science, St. Petersburg Branch, 30, 1st Lane, Saint Petersburg 199053, Russia.
E-mail: dmitry-chalikov@yandex.ru

DOI: 10.1175/JPO-D-11-0128.1

even accounts that breaking distribution on the ocean surface is fractal (Zaslavskii and Sharkov 1987). Such features are difficult to account for in analytical theories, difficult to reproduce in numerical models, and difficult to measure.

In the past decade, however, an essential progress has been made in understanding the causes of wave breaking and quantifying the breaking probability as a function of environmental properties, first of all those of the wave field itself. For monochromatic wave trains (or quasi monochromatic: i.e., a combination of a carrier wave and small sideband perturbations), the breaking onset was identified with a limiting steepness of $Hk/2 \approx 0.44$, where H is a breaking wave crest-to-trough height and k is its wavenumber [see Brown and Jensen (2001) for linear-superposition breaking, Babanin et al. (2007) for modulational-instability breaking, and Toffoli et al. (2010) for oceanic waves]. Parameterizations of the breaking probability were suggested, based on laboratory (Babanin et al. 2007) and field (Banner et al. 2000; Babanin et al. 2001) observations. Both revealed a threshold for the breaking to start happening, in terms of the background mean steepness of wave trains/fields. For the spectral environments, such important features as the cumulative effect of the breaking at small scales were found (Babanin and Young 2005; Manasseh et al. 2006; Young and Babanin 2006).

It should be mentioned that the majority of investigations of the wave breaking in the laboratory and field were conducted for the breaking stage past the breaking onset (e.g., Holthuijsen and Herbers 1986; Xu et al. 1986; Jessup et al. 1997; Gemmrich and Farmer 1999; Melville and Matusov 2002; Kleiss and Melville 2011; among many others), whereas the majority of analytical and numerical research was conducted for the incipient-breaking stage [see Longuet-Higgins (1969), Srokosz (1986), Yuan et al. (1986), Papadimitrakis (2005), and others for probability models and Banner and Tian (1998), Song and Banner (2002, hereafter SB02), and Irisov and Voronovich (2011) for numerical models]. This is due to apparent reasons. In the experiment, the whitecapping signature or its derivatives, such as underwater sound, void fraction, infrared surface trace, and radar reflection, is typically used to detect the breaking events, and otherwise it is difficult to judge on whether the wave will be breaking. The theory, on the contrary, cannot describe the complicated nature of multiphase fluid mechanics of rapid wave collapse and concentrates either on dynamics of nonlinear wave evolution to the point where the collapse starts or on interpreting statistical properties of such a point. We should note, however, that physics of the prebreaking and postbreaking evolution is essentially different: the former is nonlinear wave dynamics and the latter is water surface collapse. In this paper, we will be only dealing with the prebreaking stage and analyzing the wave evolution to the breaking onset and the onset itself, but not the breaking past this onset, when the wave starts exhibiting the whitecapping.

Because the conclusion was drawn that a wave is to reach the limiting steepness in order to break, at least in the deep water, then any physical mechanism that can lead to such steepness will result in a breaking. There can be many such mechanisms: that is, wave focusing or superposition, modulational instability, modulation of short waves by longer waves in the spectral environments, strong wind forcing, interactions of waves with currents, and interactions of waves with the bottom. The latter four are specific to wave scales or environmental conditions, and the former two are general and can occur in deep-water no-forcing circumstances.

If so, the question was, which of the two would be more frequent in field conditions? Babanin et al. (2011) argued that the superposition of waves, with the typical field wave steepness on the order of $Hk/2 \approx 0.1$, is possible, but its probability is very low in the field. Besides, signatures of the breaking allow us to distinguish between the focusing and instability-breaking types. For example, the above-mentioned mean-steepness threshold cannot be a feature of the superposition-caused breaking. This argument is indirect, but many other signatures point to the modulational instability more directly. These are double breaking (Donelan et al. 1972), upshift of the spectral energy prior to the breaking, oscillations of wave skewness/asymmetry, and the cumulative effect, which were observed in the field, but in laboratory-simulated breaking they clearly associate with the modulational instability (Babanin et al. 2010).

The modulational instability, however, is expected to be impaired or even suppressed in directional wave fields, as opposed to unidirectional wave trains typically used in wave flumes (Onorato et al. 2009a,b; Waseda et al. 2009). To investigate this issue, a dedicated experiment was conducted in a three-dimensional (3D) wave tank, with the waves quasi monochromatic in frequency domain, but with a broad range of wave-steepness and directional-distribution values (Babanin et al. 2011). The result was encouraging: for wave trains with steepness and directional spread typical of those in the ocean, the modulational instability was still active.

The present paper is the first attempt to investigate evolution of waves to breaking and the breaking onset in an environment with full wave spectrum, based on full nonlinear equations. The study is conducted by means of fully nonlinear one-dimensional potential model of Chalikov and Sheinin (1998, hereafter CS98) and Chalikov and Sheinin (2005, hereafter CS05). This model is based on first principles, proved stable and conserving energy over up to 1000 wave periods of integration, and does not have limitations in terms of wave steepness. It has been extensively used for numerical simulations of evolution to breaking in monochromatic and quasi-monochromatic wave trains and demonstrated excellent corroboration with laboratory experiments. A relevant description of this model is given in section 2. Section 3 outlines present setup of numerical experiments, and section 4 provides the main results of the paper. Conclusions and discussion items are summarized in section 5.

2. Mathematical model

Consider the periodic one-dimensional deep-water waves, whose dynamics is described by principal potential equations. No wind forcing is applied here. Because of the periodicity condition, the conformal mapping for infinite depth can be represented by the Fourier series (see details in CS98 and CS05),

$$x = \xi + \sum_{-M\le k<M, k\ne 0} \eta_{-k}(\tau)\exp(k\zeta)\vartheta_k(\xi) \quad \text{and} \tag{1}$$

$$z = \zeta + \sum_{-M\le k<M, k\ne 0} \operatorname{sign}(k)\eta_k(\tau)\exp(k\zeta)\vartheta_k(\xi), \tag{2}$$

where x and z are Cartesian coordinates; ξ and ζ are conformal surface-following coordinates; τ is time; η_k are the coefficients of Fourier expansion of the free surface $\eta(\xi,\tau)$ with respect to the new horizontal coordinate ξ,

$$\eta(\xi,\tau) = h[x(\xi,\zeta=0,\tau), t=\tau] = \sum_{-M\le k\le M} \eta_k(\tau)\vartheta_k(\xi); \tag{3}$$

ϑ_k denotes the functions

$$\vartheta_k(\xi) = \begin{cases} \cos k\xi, & k \ge 0 \\ \sin k\xi, & k < 0 \end{cases}; \tag{4}$$

and M is a truncation number.

Because of conformity, the Laplace equation retains its form in (ξ,ζ) coordinates. It is shown in CS98 and CS05 that potential wave equations can be represented in the new coordinates as follows:

$$\Phi_{\xi\xi} + \Phi_{\zeta\zeta} = 0, \tag{5}$$

$$z_\tau = x_\xi \xi_t + z_\xi \varsigma_t, \quad \text{and} \tag{6}$$

$$\Phi_\tau = \zeta_t \Phi_\xi - \frac{1}{2}J^{-1}(\Phi_\xi^2 - \Phi_\zeta^2) - z + p_0, \tag{7}$$

where (7) and (8) are written for the surface $\zeta = 0$ [so that $z = \eta$, as represented by expansion (1)]; J is the Jacobian of the transformation,

$$J = x_\xi^2 + z_\xi^2 = x_\zeta^2 + z_\zeta^2; \tag{8}$$

ζ_t is defined from the continuity equation

$$\zeta_\tau = -(J^{-1}\Phi_\zeta)_{\zeta=0}; \tag{9}$$

and Fourier coefficients for ζ_t and ξ_t are connected by the expression

$$(\xi_t)_k = \operatorname{sign}(k)(\zeta_t)_{-k}. \tag{10}$$

However high the spectral resolution might be, for long-term simulations of strongly nonlinear waves one must parameterize the energy flux into the severed part of the spectrum ($|k| > M$); otherwise, the spurious energy accumulation at large wavenumbers can corrupt the numerical solution. The simple dissipation terms were added to the right sides of Eqs. (5) and (7) for achieving stability,

$$\frac{\partial \eta_k}{\partial \tau} = E_k - \mu_k \eta_k, \tag{11}$$

$$\frac{\partial \varphi_k}{\partial \tau} = F_k - \mu_k \varphi_k \tag{12}$$

(E_k and F_k are the Fourier components of the right sides of the equations), and

$$\mu_k = \begin{cases} rM\left(\dfrac{|k| - k_d}{M - k_d}\right)^2 & \text{if} \quad |k| > k_d \\ 0 & \text{if} \quad |k| \le k_d \end{cases}, \tag{13}$$

where $k_d = M/2$ and $r = 0.25$ were chosen for all the runs discussed below. Sensitivity of the results for reasonable variations of k_d and r was low. Dissipation effectively absorbs energy if wavenumbers are close to the truncation number M, with longer waves being virtually intact. The modes with wavenumbers $|k| \le k_d$ are not affected at all. Note that an increase of the truncation number M shifts a dissipation area to higher wavenumbers, so the dissipation scheme described above retains approximation of the original (nondissipative) system.

Equations (1)–(13) are written in a nondimensional form with the following scales: length L, where $2\pi L$ is a dimensional period in the horizontal; time $L^{1/2}g^{-1/2}$; and velocity potential $L^{3/2}g^{-1/2}$ (g is acceleration of gravity). The determination of scales for other variables is straightforward.

The input of energy and momentum to waves occurs through the dynamic surface pressure p_0. According to the linear theory, the Fourier components of the surface pressure p_0 are connected with those of the surface elevation through the following expression:

$$p_k + ip_{-k} = (\beta_k + i\beta_{-k})(h_k + ih_{-k}), \qquad (14)$$

where β_k and β_{-k} are the real and imaginary parts of so-called β function (i.e., the Fourier coefficients at cosine and sine, respectively). It is a traditional suggestion that both coefficients are a function of the nondimensional frequency $\Omega = \omega_k U$ (where ω_k and U are nondimensional frequency and wind velocity, respectively). It would be quite reasonable to suggest that a reference height for wind speed might be different for different frequencies; hence, the nondimensional frequency Ω could be defined in the following way:

$$\Omega = \omega_k U(\lambda_k/2) = U(\lambda_k/2)/c_k, \qquad (15)$$

where $\omega_k = |k|^{1/2}$ is the nondimensional frequency; c_k is a phase velocity of the kth mode; and U is a nondimensional wind velocity at height $\zeta = \lambda_k/2$, where $\lambda_k = 2\pi/k$ is a length of the kth mode. The approximation of the β function was constructed by Chalikov and Rainchik (2011) on a basis of coupled Wave Boundary Layer (WBL)–wave model.

The problem of the numerical scheme validation for the wave model was discussed in CS98, CS05, and Chalikov (2005). The scheme was found to be very precise: a normal accuracy of solution for a sufficiently high resolution was around 10^{-10}. It is no surprise, because the equations written in conformal coordinates become the one-dimensional evolutionary equations that can be accurately solved by means of the Fourier transform method using no local approximations. A high accuracy of the solution and preservation of the integral invariants is crucial for a numerical wave simulation, because a ratio of time scale for waves and that for the energy input and dissipation is on the order of 10^{-4}; therefore, the wave motion is highly conservative, whereas at time scales on the order of a wave period it is actually adiabatic.

The boundary condition assumes vanishing of vertical velocity in depth,

$$\Phi_\zeta(\xi, \zeta \to -\infty, \tau) = 0. \qquad (16)$$

The solution of the Laplace equation [Eq. (6)] yields to Fourier expansion, which reduces the system of Eqs. (6)–(8) to a 1D problem,

$$\Phi = \sum_{-M \le k \le M} \phi_k(\tau) \exp(k\zeta) \vartheta_k(\xi), \qquad (17)$$

where ϕ_k are Fourier coefficients of the surface potential $\Phi(\xi, \zeta = 0, \tau)$. Equations (6)–(8) and (10) constitute a closed system of prognostic equations for the surface functions $z(\xi, \zeta = 0, \tau) = \eta(\xi, \tau)$ and the surface velocity potential $\Phi(\xi, \zeta = 0, \tau)$.

For time integration, the fourth-order Runge–Kutta scheme was used. A full description of the model, the details of numerical scheme and its accuracy, and the main results obtained with the model can be found in CS98, CS05, and Chalikov (2005, 2007, 2009). Note that a model based on conformal mapping is exact. Contradiction between results of simulations and experiments can be attributed to presence of different types of deviations of ideal conditions in experiments. For example, main attention at wave generation is directed to generation of surface. However, the distribution of velocity [the second fundamental variable in Eqs. (6)–(8)] is usually not under control. In SB02, for example, it was mentioned that measured velocity field agrees with calculations with an accuracy of 2%. In fact, such a disagreement is extremely large, because the introduction of disturbances of such magnitude will affect the numerical solution very significantly. Wave dynamics is organized so well that a comparison of 1D numerical modeling with an ideal 1D laboratory modeling can highlight the applicability of potential assumption only, but all other discrepancies should be attributed to laboratory data.

3. Description of numerical experiments

Previously, the breaking was investigated with numerical models for cases when the wave field was represented by a small number of modes (Banner and Tian 1998; SB02). Irisov and Voronovich (2011) investigated breaking the continuous spectrum tail. Here, the investigation of breaking will be done for the multimode wave field corresponding to the real wave spectrum.

In this study we have applied the above method for numerical simulation of surface waves for investigation of evolution of a wave field assigned by one-dimensional version of the Joint North Sea Wave Project (JONSWAP) spectrum S_f (Hasselmann et al. 1973) for a finite fetch as a function of frequency ω,

$$S_f(\omega) = \frac{\alpha g^2}{\omega^5} \exp\left[-\beta_1\left(\frac{\omega_p}{\omega}\right)^4\right]\gamma^r, \qquad (18)$$

where $\beta_1 = 1,25$, $\gamma = 3.3$, and ω_p is a parameter whose value is close to the frequency of the spectral peak S_p. Other parameters can be expressed through ω_p,

$$r = \exp\left[-\frac{(\omega - \omega_p)^2}{2\sigma^2\omega_p^2}\right], \quad \alpha = 0.0099\Omega^{0.66},$$

$$\sigma = \begin{cases} 0.07 & \omega \le \omega_p \\ 0.09 & \omega > \omega_p \end{cases}, \qquad (19)$$

where

$$\Omega_p = \frac{\omega_p U_{10}}{g} = \frac{U_{10}}{c_p} \tag{20}$$

is a nondimensional frequency in a spectral peak and c_p is a peak phase velocity.

In the initial JONSWAP approximation, an enhancement parameter for the spectrum γ was accepted as the constant, $\gamma = 3.3$. Later, some investigators came to the conclusion that the above parameter can be a function of a fetch or peak frequency ω_p. According to Babanin and Soloviev (1998), γ increases with Ω_p: $\gamma = 1.224\Omega_p$.

The approximations (18) and (19) were rewritten in terms of the wavenumbers using a dispersion relation that is precise at least up to $3\Omega_p$ (Chalikov 2005). The nondimensional wavenumber k_p at the spectral peak is a parameter of initial conditions. To describe a low-wavenumber part of the spectrum, k_p should exceed 1, and for good approximation of the entire spectrum, as well as the spectrum spreading due to nonlinearity, k_p should be considerably smaller, if compared with the total number of modes M. Actually, k_p is a parameter of accuracy of approximation.

The initial conditions for the Fourier coefficients of a free surface $\eta(x)$ were assigned in the following form:

$$|h_k| = (2S(k)\Delta k)^{1/2}, \quad \eta_k = |h_k|\cos(\varphi_k),$$
$$\eta_{-k} = |h_k|\sin(\varphi_k), \quad k = 1, 2, 3 \ldots M_i, \tag{21}$$

where $|h_k|$ is the amplitude of the kth mode; M_i is a number of modes assigned for initial conditions; η_k, η_{-k} are the Fourier coefficients in the Cartesian coordinates; and φ_k is a random (over k and over different runs) phase distributed uniformly over the interval $(0 \div 2\pi)$. The Fourier coefficients f_k for a surface potential $f(x)$ were assigned through

$$f_k = \operatorname{sign}(k)|k|^{-1/2}a_{-k}, \quad k = -M_i, M_i. \tag{22}$$

In this study, the model was applied to investigation of breaking waves onset. More details of model, numerical scheme, and model validation can be found in our previous publications. The peak wavenumber was 16. The number of modes M was 1000, and the number of knots $N = 4000$. Because the peak wavenumber was equal to 16, this resolution was even excessive.

In conformal coordinates, the equation for 1D waves becomes very simple. It represents a unique case in geophysical fluid dynamics, when a real process can be simulated with computer accuracy, provided that the surface steepness is not too high. The increase of the local steepness often results in the development of instability and even in the overturning of sharp crests. Formally, conformal mapping exists up to the moment when the overturning volume of water touches the surface. In such an imaginary evolution, the number of Fourier modes required increases up to infinity. If some special measures are not taken, the calculations normally terminate much earlier because of the strong crest instability (Longuet-Higgins and Tanaka 1997) followed by a split of a falling volume into two phases. This phenomenon is obviously nonpotential.

4. Results of the numerical experiments

The problem of breaking has recently been a subject of extensive theoretical and experimental research (see review in Babanin 2011). The CS98/CS05 model, as a precise and fully nonlinear model that can describe wave train evolution from any set of initial conditions all the way to the breaking start, lately was extensively employed in this kind of research. Babanin et al. (2007) used it to predict the breaking onset; the prediction was then employed in a laboratory study of wave breaking. In Babanin et al. (2010), the model was used for detailed research of nonlinear properties of waves evolving to the breaking and of the characteristics of the imminent breaker; coupled with the atmospheric boundary layer model of Chalikov and Rainchik (2011), it was used for investigations of the wind influences on this evolution and on the onset. In Babanin et al. (2010), the initial conditions were uniform wave trains. Galchenko et al. (2010, 2012) employed the CS98/CS05 model to set up a variety of combinations of carrier wave and seeded perturbations, in order to achieve different instability rates. It was presumed that such different rates will lead to different breaking severity, which was confirmed in an accompanying laboratory experiment. Thus, in all these studies, simulations with the CS98/CS05 model were combined with laboratory tests and in all the cases corroboration was excellent.

The result of numerical investigations of breaking onset on a basis of the Dold–Peregrine (DP) model were published in several papers of Banner with coauthors (Banner and Tian 1998; Song and Banner 2002; Banner and Song 2002; Song and Banner 2004; Banner and Pierson 2007). All these works considered evolution of a single wave with two superimposed disturbances. Onset of breaking was recognized by development of numerical instability of solution. Such a criterion is evidently imperfect, because numerical instability can develop long before physical instability.

In our model, the onset of breaking was defined by the first appearance of a nonsingle value of surface η,

$$x(i+1) < x(i), \quad i = 1, 2, 3, \ldots, N-1. \tag{23}$$

The integration was possible to continue shortly after that moment (see CS05), but the details of this development are not a subject of this paper. After the moment when the criterion [Eq. (23)] is reached, the solution never returns to stability: the volume of fluid crossing the vertical $x(i)$ increases rapidly. Up to this moment, the conservation of the sum of potential and kinetic energy, horizontal momentum, and the volume were excellent. Contrary to criteria used in the above-mentioned works, the criterion [Eq. (23)] is exact. In all cases simulated here, the formation of ''vertical wall'' occurred in a vicinity of wave crest. When a surface approaches to a nonsingle value (at the initial stage of breaking), conservation of invariants usually still holds, but later a sharp increase of energy occurs and a further integration becomes useless. Usually, it happens just for one Runge–Kutta time step, so probably a primary cause of the numerical instability is a growth of the right side of Eqs. (6)–(8): namely, a growth of first and second derivatives. Disintegration of the solution happens mostly because of inapplicability of potential approximation and generally because of fluid dynamic equations for single-phase fluid.

When the model is set for simulation of long-time development of spectrum, the termination of run due to breaking can be prevented by introducing the algorithm of breaking parameterization, based on selective high-frequency smoothing of an interface and surface potential profile in physical space (Chalikov 2005; Chalikov and Rainchik 2010). Because the current work is devoted to investigation of breaking itself, this smoothing was disabled and each model run was terminated with a use of the criterion in Eq. (23).

It was found that, contrary to breaking in idealized conditions, in a multimode wave field the breaking is an essentially random phenomenon. An onset of the breaking depends on many poorly controlled factors. Even if the wave spectrum in initial conditions is fixed, the time up to occurrence of breaking is different for different initial set of phases ϑ_k. This effect is also clearly pronounced in a process of freak wave formation. Therefore, the statistics of breaking should be investigated in a course of large number of numerical experiments.

All calculations were done for number of modes $M = 1000$ and number of grid points $N = 4000$. The wave number in a peak of spectrum k_p is equal to 10, and the number of modes assigned in initial conditions is equal to 100. To accelerate the approach to breaking the initial conditions were generated for the JONSWAP spectrum at $\Omega_p = 2$. Hence, the phase velocity at the wave peak was twice less than wind speed, which corresponds to the case of developing waves. Time step Δt was equal to 0.0001. As many as 5000 runs with a random set of phases were performed up to termination because of breaking. The limiting time $t = 1000$ (503 periods of peak wave) was reached just in several runs, and these cases were excluded from consideration. For a detailed study of breaking, it is necessary to record a large volume of data with a very small time interval. Such recording was not possible to provide over an entire period of integration, because it takes too much computer memory. This is why the simulations were performed in two stages. In the first stages, the calculations were done up to breaking, and the recording of all data including restart was done with interval $\delta t = 5$. In second stage, the last record of restart was taken as initial conditions for continuation of runs up to breaking. In a course of these calculations, the records were stored with interval $\delta t = 0.1$, which provided a good description of breaking development. These runs will be called final runs. Each instantaneous record includes the next fields: surface elevation z; surface potential Φ; surface velocity components u_0 and w_0; their individual derivatives on time (accelerations) $(du/dt)_0$ and $(dw/dt)_0$; local surface inclination $\partial z/\partial x$; curvature $\partial^2 z/\partial x^2$; and local columnar potential e_p, kinetic e_k, and total e_t energies, which are defined as

$$e_k = \frac{1}{2}z^2, \tag{24a}$$

$$e_k = \frac{1}{2}\int_{-\infty}^{0} (\Phi_\xi^2 + \Phi_\zeta^2)J^{-1}\, d\zeta, \quad \text{and} \tag{24b}$$

$$e_t = e_p + e_k. \tag{24c}$$

For consideration of breaking the height of a wave crest above a mean level $z = 0$ does not make any sense, because wave stability depends on the overall wave height from its trough to crest. It is not easy to detect this height formally. The calculation of a vertical distance between maximum and its nearest minimum does not give the right answer, because there can be some local extremes; hence, the wave height might be underestimated. Obviously, the extreme wave must be found between large waves. That is why the height of extreme waves H_{tc} in each record $\eta(x)$ was defined here as a difference between absolute maximum $z_{max} = H_m$ and absolute minimum $z_{min} = \min\{D_d, D_u\}$ in a moving window of length L_e. The upwind trough depth D_u and downwind trough depth D_d were usually different before breaking (see fragment of wave surface in Fig. 1).

It is reasonable to define $L_e = 1.5L_P$, where L_p is a length of wave in a peak of spectrum, $L_p = 2\pi/k_p$, and k_p is the actual wavenumber in a spectral peak. The large waves with a length exceeding $1.5L_p$ were practically

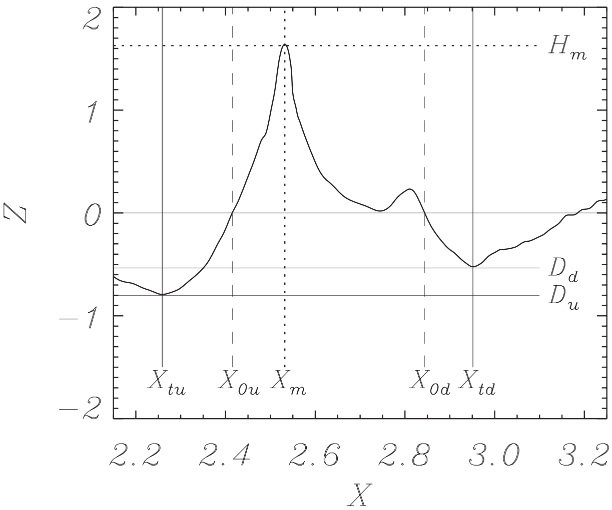

FIG. 1. Scheme used for processing of wave surface records. Here, H_m is the maximum wave height; X_m is the x coordinate of peak of such wave; D_d is the maximum depth of the front trough; X_{td} is the x coordinate of this point; D_u and X_{tu} are the same characteristics for the back trough; and X_{0d} and X_{0u} are the zero down-crossing and up-crossing points, respectively.

absent. In each record, the length of largest wave L_m can be defined as a distance between x coordinates of right X_{td} and left X_{tu} minimums, $L_m = X_{td} - X_{tu}$ (see Fig. 1). The lengths of upwind L_{mu} and downwind L_{md} slopes are defined as $L_{mu} = X_m - X_{tu}$ and $L_{md} = X_{td} - X_m$, respectively, where X_m is the x coordinate of the crest of largest wave. Note that small-scale waves introduce some uncertainty in definition of geometrical characteristics of selected wave.

The main difficulty of breaking analysis is that the largest wave during the final run (whose duration is less than 2.5 peak wave periods) can preserve its individuality only during a short period, so that the waves in different locations can play the role of largest wave in record at different moments. However, in most cases, it is the largest wave in the record that finally comes to breaking. The cases when breaking occurred without the largest waves were excluded from consideration. To investigate the evolution of the wave, tracing of the horizontal coordinate x_p of the largest wave peak was introduced, and only the waves with continuous evolution of x_p to point of breaking were selected. Remarkably, the duration of breaking development t_b is very short. The probability distribution for t_b expressed in peak wave period T_p is given in Fig. 2. As seen, the maximum of probability falls at the period $0.35T_p$. It suggests that breaking is an impulsive phenomenon, developing very quickly after the appropriate conditions arise. These conditions can be formed by reversible interactions, which are much stronger and faster than irreversible interactions. If the breaking happens, obviously the reversible interactions become irreversible.

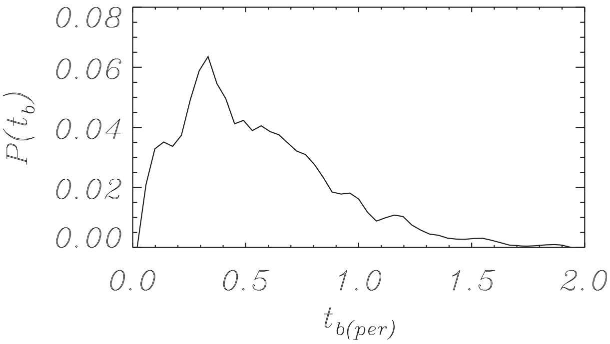

FIG. 2. Probability distribution $P(t_b)$ for period of breaking development t_b.

All the results below were obtained for the very last time period of the single largest wave evolution preceding the breaking. The runs not terminated by breaking, and the cases when the duration of the final run was less than $0.2T_p$ were excluded (in calculation of probability t_b in Fig. 2 they are accounted though).

An additional criterion of data quality was introduced by control of total energy E_t,

$$E_p = (2\pi)^{-1}\int_0^{2\pi} z^2 x_\xi \, d\xi, \tag{25a}$$

$$E_k = (2\pi)^{-1}\int_0^{2\pi} \vartheta\vartheta_\zeta \, d\xi, \quad \text{and} \tag{25b}$$

$$E_t = E_p + E_k, \tag{25c}$$

where E_k is a kinetic wave energy and E_p is a potential wave energy. In the absence of wind input and dissipation, the waves are adiabatic, but because of the slow flux of energy in subgrid part of spectrum the total energy can decrease. Variation of energy due to this effect is much slower than the increase of energy through wind input. However, if the wave surface approaches overturning, the local large gradients of elevation and surface potential cause the numerical instability, which results in a fast change the total energy. In all cases, this phenomenon took place very close to the moment when condition (23) is reached. For eliminating this effect, the cases when energy changed greater than for 0.01% were excluded. Finally, only 2260 cases were used for further analyses.

The integral probability for nondimensional crest-to-trough height H_{tc}/H_s (H_s is a significant wave height, $H_s = 4\sqrt{E_p}$) is given in Fig. 3. The sampling interval was equal to 0.1, and for calculations of probability 670 764 710 elementary events were used. As seen, the large waves

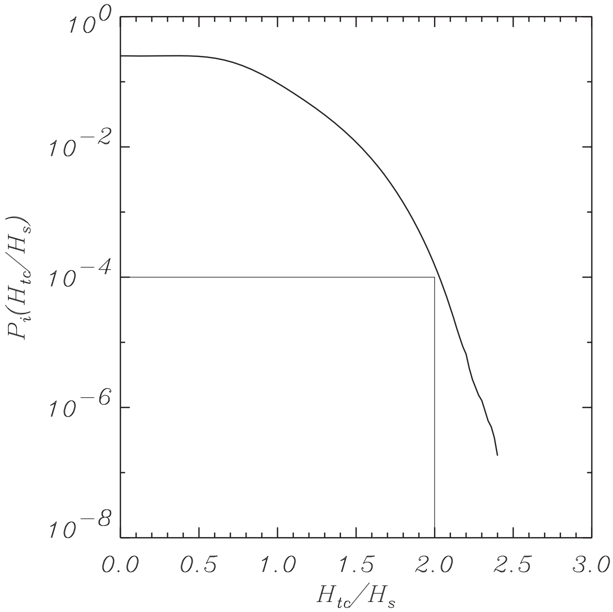

FIG. 3. Integral probability $P_i(H_{tc}/H_s)$ for trough-to-crest wave height H_{tc}, normalized by significant wave height H_s.

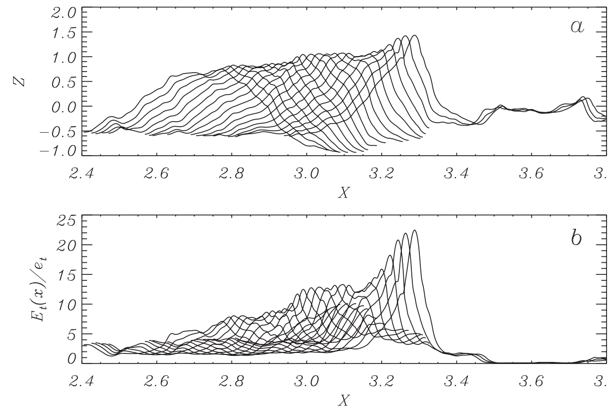

FIG. 4. (a) Example of evolution of selected wave profile z up to onset of breaking. (b) Evolution of columnar energy $e_t(x)$ [Eq. (24c)] normalized by mean energy e_t [Eq. (25c)] for the same period.

are not a too seldom phenomenon: the integral probability of waves exceeding significant wave height twice is equal to 10^{-4}; that is, one of 10 000 waves can be attributed to so-called freak waves. Because of self-similarity of equations, this result for nondimensional height is universal; however, to really be a freak wave, the wave naturally should be high enough. Note that not all freak waves break, but the portion of breaking freak waves increases with its nondimensional height H_{tc}/H_s (Chalikov 2009) and, depending on H_s and dominant wavelength, the breaking limits the maximal possible ratio H_{tc}/H_s in the field.

A typical example of wave evolution terminated by breaking is shown in Fig. 4a. As seen, the wave increases twice its crest height from $0.7H_s$ to $1.5H_s$. The depth of the back trough remains more or less the same, whereas the depth of the front trough decreases (see also Babanin et al. 2007, 2010). In Fig. 4b, the evolution of columnar energy e_c is presented. It is seen that maximum columnar energy before breaking exceeds the average energy by 8 times. More clearly, this effect is demonstrated in Fig. 5, where the time evolution of averaged over distance L_m and energy E_m is represented together with evolution of maximum value of the columnar energy E_{max}. The averaged wave energy E_m changes insignificantly and mostly because of some uncertainty in definition of L_m caused by presence of local extremes. However, the maximum of columnar energy E_{max} changes several times. It will be shown below that such growth is provided by a concentration of the energy around crest vertical. This effect was found also as a primary reason of freak wave generation (Chalikov 2009). Evidently, the breaking waves and freak waves have a similar nature. However, large wave height is not a necessary condition of breaking, because smaller waves also break. This fact signifies that in the spectral environment the breaking is not necessarily connected with overall wave characteristics but rather with rapidly changing local condition in a vicinity of wave crest.

The presented below results are obtained by processing of all 2260 final runs. The evolution of total energy of wave averaged over its length L_e and normalized by total energy E_t as function of time before breaking (expressed in peak wave periods),

$$E_m = \frac{1}{E_t L_e} \int_{L_e} e_t \, dx, \qquad (26)$$

is shown in Fig. 6a. The solid thick curve is averaged over all cases evolution of E_m, and the distance between dotted lines indicates the dispersion. As seen, the energy of the wave before breaking is close to doubled averaged

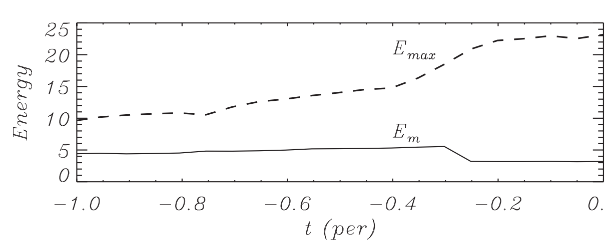

FIG. 5. Evolution of averaged over wavelength columnar energy E_m and maximum of columnar energy E_{max} for the development shown in Fig. 4.

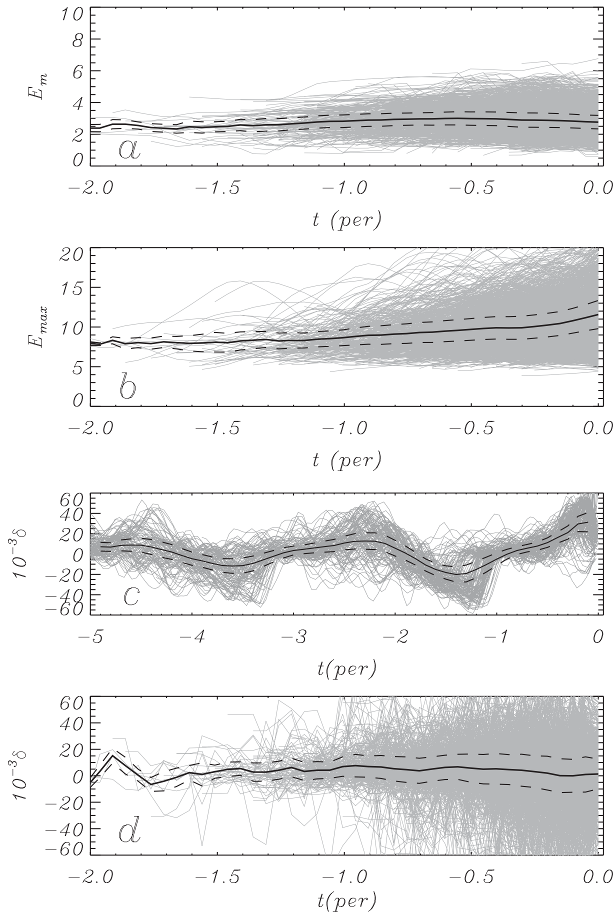

FIG. 6. (a) Evolution of the energy of selected wave E_m [Eq. (26)] averaged over wavelength L_m prior to breaking as a function of time t, expressed in peak wave periods. Aggregated gray lines correspond to single cases, the solid line represents the averaged over all cases of evolution, and dotted lines correspond to dispersion. Moment of breaking corresponds to time $t = 0$. (b) As in (a), but for maximum value $E_{\max}$ of columnar energy E_t in the selected window. (c) Evolution of δ [Eq. (28)] for idealized initial conditions. (d) Evolution of δ in spectral environment. The style of curves in (b),(c) are as in (a).

energy E_m, but it can be several times larger and smaller than E_m. The dispersion in Fig. 6a is very stable and small, on the order of 0.1. It is most interesting that on average the approach to breaking does not manifest itself by growth of wave energy. This fact confirms that a breaking wave in the spectral environment does not necessarily take the energy from other waves. In events simulated here, the developing of breaking instability occurs because of modification of its shape: wave becomes more sharp crested with concentration of its energy around its peak, the crest becomes unstable, and breaking of the wave starts. It is demonstrated clearly in Fig. 6b, where the evolution of maximum columnar energy $\max(e_t)$ is shown. As seen, the maximum energy increases on average by 1.5 times, though individual growth can reach a value of 3. Note that in developing extreme (freak) waves the amplification of maximum energy can reach such a large value as 10. Therefore, the level of energy is not an indicator of breaking. Banner and Tian (1998) suggested that the onset of breaking can be recognized by the rate of growth of energy averaged over wavelength E_m,

$$\beta_E = \frac{1}{\omega E_m}\frac{dE_m}{dt}. \tag{27}$$

The behavior of this parameter was investigated with the numerical model of Dold (1992) based on a surface integral method. In the initial condition, one harmonic carrying wave and two small-amplitude disturbances were assigned and the evolution of energy of the carrying wave was investigated. It was assumed that, after development of modulation instability, the approach to breaking can be recognized by exceeding the parameter β_E by some critical value. In fact, even for such a highly idealized situation, SB02 found that parameter β_E ''did not provide a robust indicator for resolving the onset of breaking'' (SB02, p. 2547). This is why they suggested the alternative parameter, based on maximum value of wave energy $(E_m)_{\max}$,

$$\delta = \frac{1}{\omega(E_m)_{\max}}\frac{d(E_m)_{\max}}{dt}. \tag{28}$$

In fact, replacing β_E by $(\beta_E)_{\max}$ cancels the role of modulational instability, because growth of maximum columnar energy can occur without growth of overall wave energy (see Figs. 6a,b). Finally the authors came to conclusion that their ''calculations indicate that breaking or recurrence may be determined by a common threshold $\delta_{\rm th}$ in the range $(1.3 \times 10^{-3}, 1.5 \times 10^{-3})$ for the nondimensional growth rate'' (SB02, p. 2553).

The practical role of criterion type of Eq. (28) is doubtful. First, the primary authors' idea was explanation of breaking on a basis of modulation instability, when one wave grows at the expenses of others. Criterion δ cannot describe such process, because it is based on the maximum energy of waves, which depends essentially on shape of the wave and it can change without change of energy. This effect is clearly demonstrated in Fig. 5: the average wave energy slightly decreases, whereas the peak energy increases nearly 3 times. Second, this criterion is established for idealized situation of single harmonic wave with two superimposed disturbances, and it is unclear how to apply it for parameterization of breaking in spectral models or in direct modeling of multimode wave field.

For investigation of breaking in idealized conditions, the series of experiments similar to those performed by SB02, were repeated with the CS98/CS05 model. Carrying wave mode with amplitude was placed at wavenumber $k = k_p$, where k_p changed in the range of 3–10 and steepness $k_p a_p$ changed in the range of 0.085–0.185. A total of 160 long-term simulations were done up to breaking or up to nondimensional time $t = 500$; this corresponds to 138–252 periods of carrying waves. Disturbances with amplitudes $0.1a_p$ were assigned at wavenumbers $k_p + 1$ and $k_p - 1$, which for the given resolution provided fast enough growth of disturbances (see Chalikov 2007). The number of modes was M = 2000, and the number of grid points was N = 8000: that is, a sufficient accuracy of approximation was maintained. These series of numerical experiments were initially intended for investigation of breaking, but then we concentrated on simulation of breaking in spectral environments. A criterion for terminating a run was defined by Eq. (23).

The evolution of δ [Eq. (28)] prior to wave breaking for such idealized wave field is shown in Fig. 6c. Gray curves correspond to evolution of δ in individual runs, the solid line corresponds to averaged evolution, and dashed lines indicate variance. Time t is normalized by the period of carrying waves. As seen, for the less-steep waves, the DP model performs reasonably well and the behavior of δ in an idealized condition reminds us slightly of the quasi-periodic regime obtained by SB02. The evolution of δ, however, is less regular than it was demonstrated in SB02, because the simulated wave field has been modified because of the appearance of new modes. The current calculation shows that criterion δ can exceed the recommended values $\delta_{th} = 0.7 \times 10^{-3}$–$2.8 \times 10^{-3}$ at least for one decimal order. It means that an exact model based on conformal transformation is much more stable, so the recurrence occurs after reaching of large values of δ. Note that breaking can also occur at very small values of δ.

The data on δ obtained in analogous simulation of breaking in spectral environment are shown in Fig. 6d. As seen, the data on evolution of δ exhibit a great scatter. It is not surprising, because δ is an overall characteristic and for complicated wave surface its value is very sensitive to definition of wavelength L_m. Besides, the height of sharp-crested wave approaching breaking in the spectral environment can change very quickly, and criterion (28) demonstrated irregular fluctuations. The parameter δ can obtain negative and positive values, exceeding many times the above-mentioned limit δ_{th}. These results suggest that even modified formulation of breaking criterion [Eq. (28)] cannot describe the variety of situations. Note that data in Fig. 6d characterize the period just prior to breaking. However, large values of criterion δ occur very often when growth of wave energy is reversible. The probability distribution of δ obtained for all runs over the entire period of integration is shown in Fig. 7. As seen, the probabilities of negative and positive values of δ are approximately equal each to other, and its absolute value can greatly exceed δ_{th}. Note that part of the breaking cases in Fig. 7 is less than 0.001%.

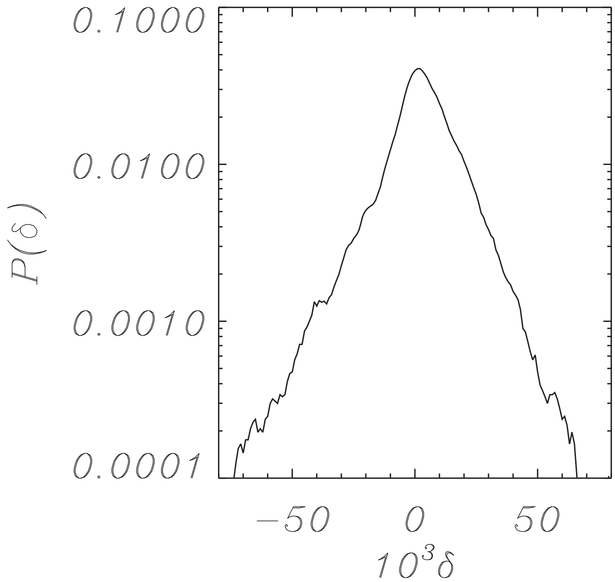

FIG. 7. Probability distribution for criterion δ [Eq. (28)].

Therefore, we come to a conclusion that criterion δ does not signify a breaking, and waves are much more stable than those reproduced by models that were used in cited papers. Hence, investigation of role of input energy to waves and vertical gradient of mean velocity performed by SB02 on a basis of the criterion in Eq. (27) was premature. Actually, the DP model is an excellent tool for investigation of wave dynamics, when steepness is not too large, but it is inapplicable for investigation of extreme conditions of breaking. Hence, it is most likely that the papers cited above discussed not the breaking instability but the limits of numerical stability of the model used. The CS98/CS05 model used in our calculation is able to precisely reproduce the dynamics of extremely steep waves [see long-term simulations of Stokes waves in CS05 and Chalikov (2005)]. The criterion in Eq. (23) is exact because, up to the moment of the vertical wall appearing, the accuracy of solution is very high.

Some investigators (see, e.g., Zakharov et al. 2006) suggested that breaking occurs because of reaching the limit form of Stokes waves $H_{tc}/2L_m = 0.43.$, where L_m is the length of wave. The evolution of the height of largest

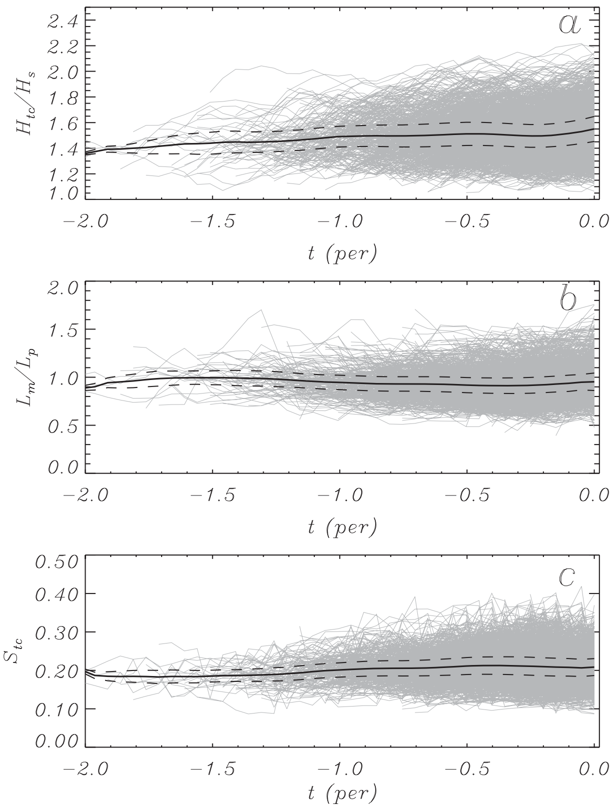

FIG. 8. (a) Evolution of trough-to-crest wave height H_{tc} normalized by H_s prior to breaking as function of time t. (b) Evolution of ratio of actual wavelength L_m to spectral wavelength of peak wave L_p. (c) Evolution of overall steepness S_{tc}. The styles of curves are as in Fig. 6.

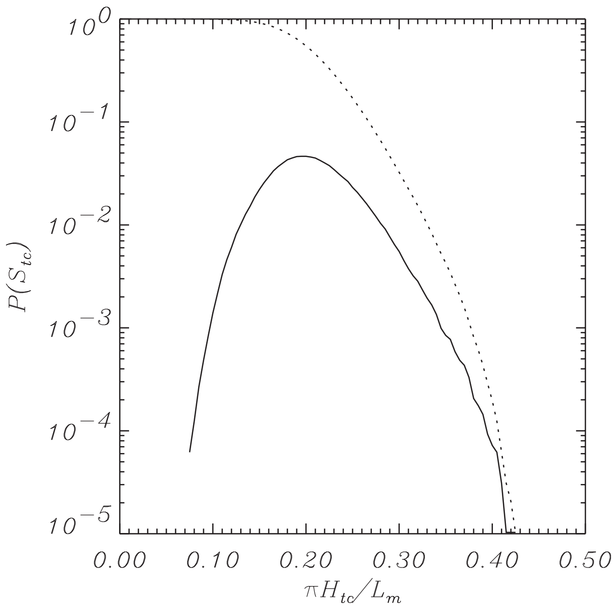

FIG. 9. Probability distribution for criterion overall steepness S_{tc}.

trough-to-crest wave height H_{tc} normalized by significant wave height is given in Fig. 8a. The growth of the averaged height occurs only in the last stage and has the order of $0.2H_s$. As seen, the breaking occurs in a wide range of H_{tc}/H_s between values 1.0 and 2.5, so the trough-to-crest height of wave cannot serve as an indicator for wave breaking, though the increase of H_{tc}/H_s is always followed by growth of breaking probability (Chalikov 2007). In the multimode wave field, the length L cannot be defined straightly, because the largest peak wave is distorted by smaller waves. The evolution of L_m, normalized by spectral peak wavelength $L_p = 2\pi/k_p$ is given in Fig. 8b, which proves that, on average, the wavelength changes insignificantly with weak tendency to decrease by 10%. This effect was confirmed by SB02. However, the scatter of these data is very large. Data on the overall steepness $S_{\mathrm{tc}} = H_{\mathrm{tc}}/2L_m$ of the largest wave prior to breaking are given in Fig. 8c. It is seen that just several waves break at high overall steepness $S_{\mathrm{tc}} = 0.4$, but breaking also occurs at such small steepness as $S_{\mathrm{tc}} = 0.1$. The averaged steepness of breaking waves is not too small and equal to 0.2, but it is twice smaller than critical steepness for Stokes waves. The gray curves, corresponding to individual cases are concentrated very close to averaged curve, and very small dispersion of the results (shown by dotted curves) proves that scatter of wave steepness prior to breaking is very small. Therefore, the overall steepness of waves is also not a criterion of wave breaking. The probability distribution of overall steepness shown in Fig. 9 testifies that waves in spectral environment break well in advance before they become very steep. It can be concluded that in multimode wave field the parameter of overall steepness S_{tc} is not a reliable criterion for recognizing breaking.

Important characteristics of wave shape closely connected with wave breaking is the wave asymmetry A_s, which is defined as (see Fig. 1)

$$A_s = \frac{X_{0d} - X_m}{X_m - X_{0u}} \tag{29}$$

(Tulin and Landrini 2001; Caulliez 2002; Young and Babanin 2006; Babanin et al. 2007, 2010). The negative asymmetry $A_s < 0$ corresponds to a wave tilted forward in the direction of propagation. In Fig. 1, the wave has large positive asymmetry because of a secondary peak on the downwind wave slope. This example confirms that estimation of overall wave characteristics is often connected with uncertainty. The evolution of asymmetry prior to breaking is shown in Fig. 10a for calculations with a small number of modes. These calculations prove that in an idealized wave field the waves have a negative asymmetry. An analogous analysis of data obtained in

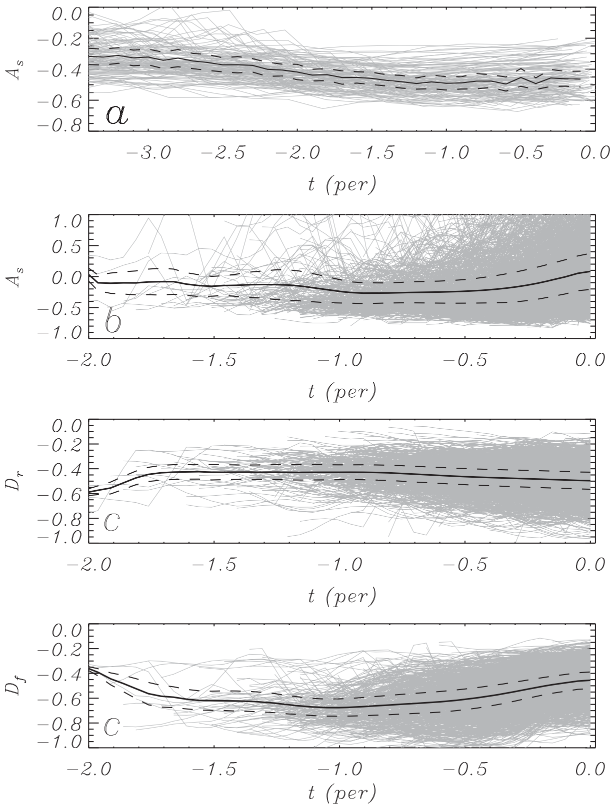

FIG. 10. (a) The evolution of asymmetry A_s [Eq. (29)] prior to breaking as a function of time t, expressed in peak wave periods. (b) The same characteristics obtained in calculation for spectral environment. (c) Evolution of upwind rear depth D_u normalized by H_s. (d) Evolution of the front trough depth D_u normalized by H_s. The styles of curves are as in Fig. 6.

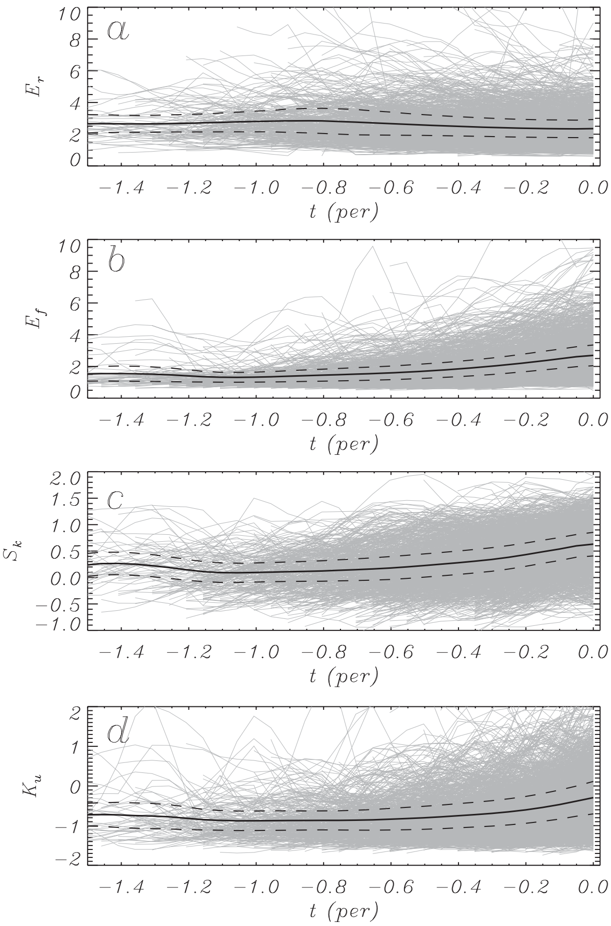

FIG. 11. The evolution of geometrical characteristics prior to breaking: (a) the ratio of wave height above mean level to depth of the rear trough D_r; (b) the ratio of wave height above mean level to depth of the rear trough D_f; (c) skewness S_k of waves; and (d) the kurtosis K_u of waves.

spectral environment shown is given in Fig. 10b. As seen, the asymmetry has a very large scatter changing from -0.9 to values exceeding 1. On average, waves have a slight negative asymmetry, but just before the breaking asymmetry change sign and become positive. This effect can be explained by sharp modification of wave shape before breaking (similar to that shown in Fig. 1).

Kjeldsen and Myrhaug (1980) found that the front trough of the incipient breaker is shallower compared to the rear trough, which is a persistent feature of wave breaking observed in the laboratory (Babanin et al. 2010). This was confirmed by calculations with idealized wave field, but the data obtained in spectral environment contradict this conclusion: the front trough D_f of breaking waves (Fig. 10b) is on average deeper than the rear trough D_r (Fig. 10c). Note that both characteristics have a large scatter.

The theoretical analysis of breaking is usually based on presentation of wave field as a superposition of harmonic waves. Such restriction leads to the assumption that that one mode grows, taking the energy from other modes. If the number of modes is small, such a transformation occurs within the length of the wave group. In a case of wind sea spectrum, such an interval does not exist, so we should suppose that growth of energy leading to breaking occurs everywhere in the area represented by the wave spectrum. In reality, just a few waves grow and break in physical space, and this process is represented in the wave spectrum in a highly distorted form. A shape of wave approaching to breaking is very far from a harmonic function. It is illustrated in Fig. 11, where the ratio of wave height above the mean level to the rear trough (Fig. 11a) and to the front trough (Fig. 11b) is represented. As seen, wave height is twice larger than the depth of troughs, and the depth of the front trough on average is slightly deeper than the depth of the rear trough (see also Babanin et al. 2007, 2010).

This effect is confirmed by Figs. 11c,d, which represented the skewness S_k and kurtosis K_u calculated over wavelength L_m. As seen, the skewness of waves is on average is positive; hence, the crests are considerably higher than the depth of the troughs. Kurtosis on average is negative, which means that areas with positive elevation are less extended than areas with negative elevation.

In fact, we came to the conclusion that no single characteristic considered provides a reliable criterion for wave breaking in a spectral environment. Note also the scatter with respect to the mean. All considered properties can be referred rather to overall characteristics, whose definition is very sensitive to real shapes of waves and strongly depends on spectral resolution and the shape of the spectrum. Not one of these characteristics [including the nondimensional rate of wave height growth; Eq. (28)] can be considered as a reliable criterion of breaking onset. If anything, it is rather local slope near the crest, as outlined below.

Considering Figs. 6a,b,d; 8a–c; and 10a–c, we can conclude that, contrary to idealized conditions (see Fig. 6c), the simple geometrical characteristics are very unstable. The shape of peak waves can be distorted by smaller waves; therefore, the values of wave height and wavelength, overall steepness S_{tc}, and asymmetry A_s can depend on small details. It explains the large scatter of these characteristics.

Now, we consider the evolution of local characteristics of wave approaching to breaking: maximum s_{max} and minimum s_{min} slope in the interval $L_m = X_{td} - X_{tu}$ (Figs. 12a,b). As seen, the positive steepness (i.e., steepness at rear slope) changes insignificantly, whereas steepness at the front slope can reach very large negative values. An even more clear characteristic is the sharpness of wave peak, which is characterized by maximum value of the second derivative (Fig. 12c). Note that the value of the second derivative is multiplied by H_s to make these characteristics independent of model parameters. In the numerical model, the value of second derivative could reach several thousands, which forced us to modify the time step. However, all differential characteristics reveal the large scatter: breaking could occur at large and small steepness and at large and small negative peak sharpness. The attempts to find the threshold value for negative steepness were unsuccessful: the process can be reversible up to very large values of s_{min}, and only the appearance of a nonunique surface (in fact the onset of breaking itself) can be accepted for sure as a criterion of breaking. The same comments can be attributed to kinematic characteristics of surface: the maximum and minimum values of component of surface orbital velocity (Figs. 13a–d) and components of acceleration (individual derivatives of velocity) dU/dt and dW/dt

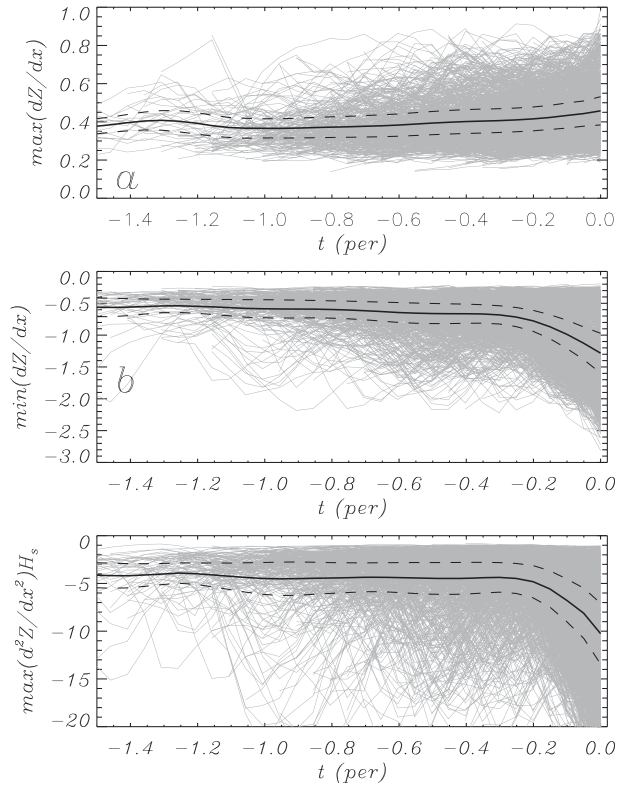

FIG. 12. Differential characteristics of surface: (a) the evolution of maximum value of steepness $\max(\partial z/\partial x)$; (b) the evolution of minimum value of steepness $\min(\partial z/\partial x)$; and (c) the evolution of minimum value of curvature $\min(\partial^2 z/\partial x^2)H_s$ taken with opposite sign. The styles of curves are as in Fig. 6.

(Fig. 14). The deceleration of horizontal velocity (Fig. 14b) and acceleration of negative vertical velocity (Fig. 14c) are most clearly pronounced. Again, the scatter of these characteristics is very large.

Finally, we come to the conclusion that all considered characteristics cannot serve as criteria of breaking development. Some of them exhibit the tendency to instability, but these features are developing during a very short period preceding breaking, so they correspond to the process of breaking itself rather than they prescribe the imminent breaking.

After such a detailed consideration of breaking process, we have a right to ask the following question: How is it possible to use a predictor for breaking in the spectral environment? Definitely, instability of interface leading to breaking is an important problem of fluid mechanics. This process is strongly nonlinear, and theory of breaking is expected to be highly complicated. The onset of breaking is analogous to the onset of free convection in a liquid at unstable stratification. The criterion of convection instability is just an appearance of the unstable stratification in some part of liquid. It can

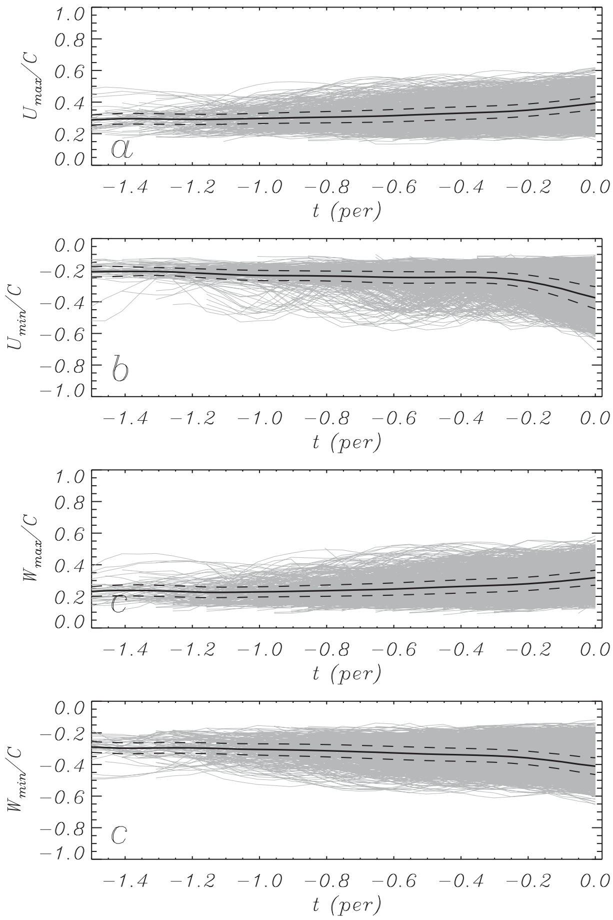

FIG. 13. The evolution of surface kinematic characteristics: (a) the evolution of maximum value of horizontal velocity $U_{\max}/c_p$; (b) the evolution of minimum value of horizontal velocity $U_{\min}/c_p$; (c) the evolution of maximum value of vertical velocity $W_{\max}/c_p$; and (d) the evolution of minimum value of vertical velocity $W_{\min}/c_p$. All velocities are normalized by peak phase velocity c_p.

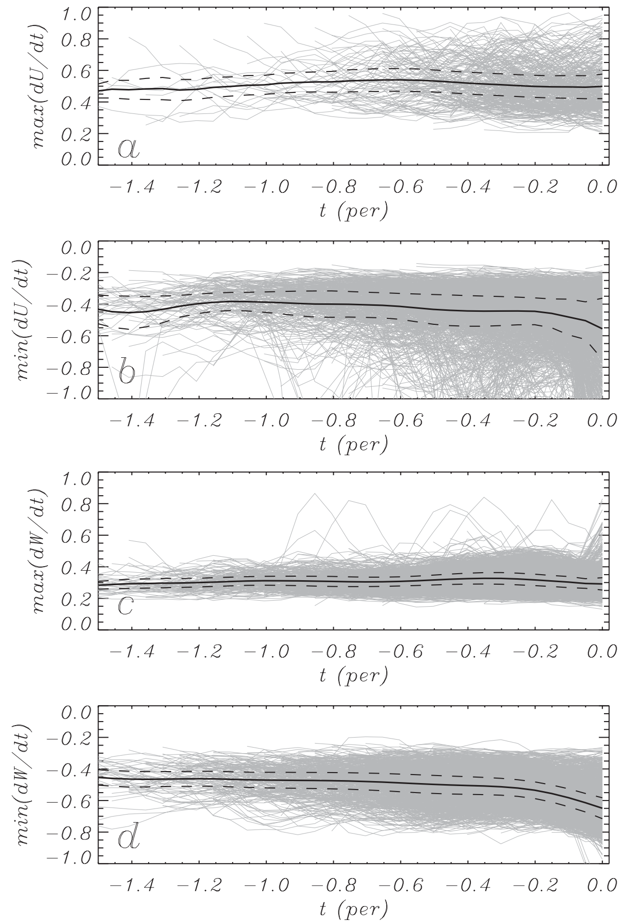

FIG. 14. The evolution of surface dynamic characteristics (accelerations normalized by acceleration of gravity): (a) the evolution of maximum value of horizontal particle acceleration $\max(dU/dt)g^{-1}$; (b) the evolution of minimum value of horizontal particle acceleration $\min(dU/dt)g^{-1}$; (c) the evolution of maximum value of vertical particle acceleration $\max(dW/dt)g^{-1}$; and (d) the evolution of minimum value of vertical particle acceleration $\min(dW/dt)g^{-1}$.

result from different processes, producing the redistribution of density. By analogy, we can define a criterion of instability as the appearance of a nonunique part of surface, when some volume of fluid becomes unsupported by pressure from the surrounding liquid and started to move independently under the forces of inertia and gravitation. The breaking can start under the influence of many factors, producing the nonuniqueness of surface. Probably, the main factor is the appearance of horizontal velocity exceeding the velocity of shape propagation. It was confirmed in the special numerical experiments with very high time and space resolution performed by CS05. It was shown that horizontal velocity in a peak of wave before breaking always exceeded the phase velocity.

The breaking is a dissipative process, leading to loss of kinetic and potential wave energy and transition of energy to the current and turbulence, so it should be taken into account in different types of models designed for simulation of wave evolution. The most important models of such type are wave-forecasting models (e.g., the Wavewatch model; Tolman 2008). Evidently, any criterion of breaking cannot be used in such models, because they operate with wave spectrum, and the information on real wave surface is absent. In such models, the dissipation process is presented in a distorted form. Because breaking occurs in relatively narrow space intervals separated by broad parts with no breaking, the spectrum of dissipation rate is distributed mostly in the high-frequency part of the spectrum, whereas in reality the breaking reduces the height of the largest wave represented in a spectral peak. The reason for this contradiction is that, in the spectral model the wave field is assumed to be a superposition of linear modes, whereas breaking (and growth of freak waves) occurs because of transformation of a specific wave shape: wave before breaking as a rule becomes sharp crested. Therefore, the breaking reduces the height and energy of nonlinear waves.

5. Conclusions

In this paper, the exact two-dimensional model was used for investigation of breaking onset, which was recognized as appearance of the nonuniqueness of surface. This criterion is strict, because up to this moment of the wave evolution the conservation of integral is supported with high precision and after this moment the breaking is imminent. Because of the special strategy of numerical experiments and archiving the results, the evolution of wave approaching the breaking was registered with high accuracy. This last period prior to the breaking was a subject of investigation. The analysis of results allowed us to formulate the following conclusions:

1) Contrary to considerations based on a small number of modes, the definition of the wave in a spectral environment is less certain. In reality, the wave is a composition of many modes with more or less fixed phases. Because of dispersion, the wave surface represents a complicated shape. This is why defining an individual wave is also uncertain. Statistical characteristics of such a wave usually have large scatter.
2) The spectral approach to investigation of breaking waves is misleading, because the breaking occurs in a narrow interval of physical space and its spectral image is difficult to interpret.
3) The mechanism of breaking in a spectral environment is quite different than that for idealized situations when the wave field is represented by a few modes.
4) The breaking develops very quickly, on average faster than for half of a peak wave period. The breaking at some degree is analogous to development of freak waves, which generally appear suddenly without any prehistory. Probably, a main reason of such development can be reversible wave–wave interaction.
5) There was found no robust predictor for breaking in the spectral environment threshold or limiting value of some global wave parameters, which indicate the imminent breaking. Calculations with exact model show that criterion based on rate of maximum energy can be exceeded many times. This means that real process is much more stable than it was demonstrated in Song and Banner (2001), where the breaking onset was identified with development of numerical instability. The overall characteristics of breaking (e.g., overall steepness, asymmetry, overall kurtosis, and skewness) reveal a weak connection with breaking process.
6) The differential geometrical and kinematical characteristics like first and second derivatives of elevation, surface orbital velocity, and individual accelerations [as well as criterion δ; Eq. (28)] indicate a development toward breaking clearer, but they rather describe the process of breaking itself than predict its onset. At another similar situation, the development does not necessarily result in a breaking: at some moment before the breaking the process can become reversible.

The most striking property of wave breaking in spectral environment is the absence of any evident rules and criteria for breaking onset. We can be only sure that breaking starts, in most cases, at the front slope of the wave very close to its peak. The breaking occurs as a result of local instability of flow in areas with large negative steepness. It is followed as a rule by deceleration of the horizontal component of surface orbital velocity and negative acceleration of the vertical component of vertical velocity.

The breaking process develops in intervals that are much shorter than dominant wavelength. For spectral description of such modification, the high-frequency (wavenumbers) modes are needed. However, in reality, the breaking decreases the energy of a large wave, by changing its shape. Generally, the spectral approach is not fully applicable to analysis of individual breaking cases, which occur in a physical space and cause an unclear transformation of wave spectrum.

The role of the modulational instability in wave fields with a continuous spectrum has to also be mentioned here. As discussed in the introduction, this is the most likely cause of dominant breaking in quasi-monochromatic wave trains, and in such trains it leads to steepness of $Hk/2 \approx 0.44$ at the breaking onset. Such a limiting steepness was also observed in directional wave fields, and in fact this is the maximal steepness of the imminent breaker in simulations of the present paper (Fig. 8). In this regard, results of this paper agree with one-dimensional simulations of the modulational instability and with the field observations; that is, if a wave reaches such steepness, it will definitely break.

The main difference is that in the spectral environments surface of waves can become unstable and collapse at much lower global steepness. This apparently happens because of reasons discussed in conclusion 5 above, and such distortions of the wave shape and of the regular course of the wave evolution, as well as of the modulational instability on that matter, would trigger the breaking earlier. These distortions also seem very likely in case of random superposition of waves of all scales. It is likely but not inevitable, and a wave can in fact proceed all the way to the limiting steepness found in the clear evolution of modulated wave trains. This fact indicates that the modulational instability remains active in the spectral environments, at least in the range of steepness considered. Then, the presence of the modulation instability allows us to explain the observation of multiple signatures of wave breaking in oceanic fields, which associate such breaking with the modulational instability as discussed in the introduction.

Acknowledgments. D. Chalikov and A. Babanin conducted this research with the support of a research development scheme (RDS) grant of the Swinburne University of Technology. The authors wish to thank anonymous reviewers for many useful comments.

REFERENCES

Babanin, A. V., 2011: *Breaking and Dssipation of Ocean Surface Waves.* Cambridge University Press. 463 pp.

——, and Yu. P. Soloviev, 1998: Investigation of transformation of the wind wave frequency spectrum with fetch and the stage of development. *J. Phys. Oceanogr.,* **28,** 563–576.

——, and I. R. Young, 2005: Two-phase behavior of the spectral dissipation of wind waves. *Proc. Fifth Int. Symp. on Ocean Wave Measurement and Analysis,* Madrid, Spain, CEDEX and ASCI CORPI, 51.

——, ——, and M. L. Banner, 2001: Breaking probabilities for dominant surface waves on water of finite constant depth. *J. Geophys. Res.,* **106,** 11 659–11 676.

——, D. Chalikov, I. Young, and I. Savelyev, 2007: Predicting the breaking onset of surface water waves. *Geophys. Res. Lett.,* **34,** L07605, doi:10.1029/2006GL029135.

——, ——, ——, and ——, 2010: Numerical and laboratory investigation of breaking of steep two-dimensional waves in deep water. *J. Fluid Mech.,* **644,** 433–463.

——, T. Waseda, T. Kinoshita, and A. Toffoli, 2011: Wave breaking in directional fields. *J. Phys. Oceanogr.,* **41,** 145–156.

Banner, M. L., and X. Tian, 1998: On the determination of the onset of breaking for modulating surface gravity waves. *J. Fluid Mech.,* **367,** 107–137.

——, and J.-B. Song, 2002: On determining the onset and strength of breaking for deep water waves. Part II: Influence of wind forcing and surface shear. *J. Phys. Oceanogr.,* **32,** 2559–2570.

——, and W. L. Peirson, 2007: Wave breaking onset and strength for two-dimensional and deep-water wave groups. *J. Fluid Mech.,* **585,** 93–115.

——, A. V. Babanin, and I. R. Young, 2000: Breaking probability for dominant waves on the sea surface. *J. Phys. Oceanogr.,* **30,** 3145–3160.

Bortkovskii, R. S., 1987: *Air-Sea Exchange of Heat and Moisture during Storms.* D. Riedel, 194 pp.

Brown, M. G., and A. Jensen, 2001: Experiments in focusing unidirectional water waves. *J. Geophys. Res.,* **106,** 16 917–16 928.

Caulliez, G., 2002: Self-similarity of near-breaking short gravity wind waves. *Phys. Fluids,* **14,** 2917–2920.

Cavaleri, L., and Coauthors, 2007: Wave modelling—The state of the art. *Prog. Oceanogr.,* **75,** 603–674.

Chalikov, D., 2005: Statistical properties of nonlinear one-dimensional wave fields. *Nonlinear Processes Geophys.,* **12,** 1–19.

——, 2007: Numerical simulation of Benjamin-Feir instability and its consequences. *Phys. Fluids,* **19,** 016602, doi:10.1063/1.2432303.

——, 2009: Freak waves: Their occurrence and probability. *Phys. Fluids,* **21,** 076602, doi:10.1063/1.3175713.

——, and M. Belevich, 1993: One-dimensional theory of the wave boundary layer. *Bound.-Layer Meteor.,* **63,** 65–96.

——, and D. Sheinin, 1998: Direct modeling of one-dimensional nonlinear potential waves. *Nonlinear Ocean Waves,* W. Perrie, Ed., Advances in Fluid Mechanics, Vol. 17, Computational Mechanics Publications, 207–258.

——, and ——, 2005: Modeling of extreme waves based on equations of potential flow with a free surface. *J. Comput. Phys.,* **210,** 247–273.

——, and S. Rainchik, 2011: Coupled numerical modelling of wind and waves and theory of the wave boundary layer. *Bound.-Layer Meteor.,* **138,** 1–41.

Dold, J. W., 1992: An efficient surface-integral algorithm applied to unsteady gravity waves. *J. Comput. Phys.,* **103,** 90–115.

Donelan, M. A., M. S. Longuet-Higgins, and J. S. Turner, 1972: Periodicity in whitecaps. *Nature,* **239,** 449–451.

Galchenko, A., A. V. Babanin, D. Chalikov, I. R. Young, and T.-W. Hsu, 2010: Modulation depth and breaking strength for deep-water wave groups. *J. Phys. Oceanogr.,* **40,** 2313–2324.

——, ——, ——, ——, and B. K. Haus, 2012: Influence of wind forcing on modulation and breaking of one-dimensional deep-water wave groups. *J. Phys. Oceanogr.,* **42,** 928–939.

Gemmrich, J. R., and D. M. Farmer, 1999: Observations of the scale and occurrence of breaking surface waves. *J. Phys. Oceanogr.,* **29,** 2595–2606.

Hasselmann, K., and Coauthors, 1973: Measurements of wind-wave growth and swell decay during the Joint North Sea Wave Project (JONSWAP). Deutches Hydrographisches Institut Rep. 12, 93 pp.

Holthuijsen, L. H., and T. H. C. Herbers, 1986: Statistics of breaking waves observed as whitecaps in the open sea. *J. Phys. Oceanogr.,* **16,** 290–297.

Irisov, V., and A. Voronovich, 2011: Numerical simulation of wave breaking. *J. Phys. Oceanogr.,* **41,** 346–364.

Jessup, A. T., C. J. Zappa, M. R. Lowen, and V. Hesany, 1997: Infrared remote sensing of breaking waves. *Nature,* **385,** 52–55.

Kerman, B. R., 1992: *Natural Physical Sources of Underwater Sound: Sea Surface Sound.* Kluwer Academic, 749 pp.

Kjeldsen, S. P., and D. Myrhaug, 1980: Wave-wave interactions, current-wave interactions and resulting extreme waves and breaking waves. *Proc. 17th Int. Conf. on Coastal Engineering,* Sydney, Australia, ASCE, 2277–2303.

Kleiss, J. M., and W. K. Melville, 2011: The analysis of sea surface imagery for whitecap kinematics. *J. Atmos. Oceanic Technol.,* **28,** 219–243.

Longuet-Higgins, M. S., 1969: On wave breaking and the equilibrium spectrum of wind-generated waves. *Proc. Roy. Soc. London,* **A310,** 151–159.

——, and M. Tanaka, 1997: On the crest instabilities of steep surface waves. *J. Fluid Mech.,* **336,** 51–68.

Manasseh, R., A. V. Babanin, C. Forbes, K. Rickards, I. Bobevski, and A. Ooi, 2006: Passive acoustic determination of wave-breaking events and their severity across the spectrum. *J. Atmos. Oceanic Technol.,* **23,** 599–618.

Melville, W. K., and P. Matusov, 2002: Distribution of breaking waves at the ocean surface. *Nature,* **417,** 58–63.

——, M. Loewen, F. Felizardo, A. Jessup, and M. Buckingham, 1988: Acoustic and microwave signatures of breaking waves. *Nature,* **336,** 54–56.

Onorato, M., and Coauthors, 2009a: Statistical properties of mechanically generated surface gravity waves: A laboratory experiment in a three-dimensional wave basin. *J. Fluid Mech.,* **637,** 235–257.

——, and Coauthors, 2009b: On the statistical properties of directional ocean waves: the role of the modulational instability in the formation of extreme events. *Phys. Rev. Lett.,* **102,** 114502, doi:10.1103/PhysRevLett.102.114502.

Papadimitrakis, Y. A., 2005: On the probability of wave breaking in deep water. *Deep-Sea Res. II,* **52,** 1246–1269.

Sharkov, E. A., 2007: *Breaking Ocean Waves: Geometry, Structure and Remote Sensing.* Springer, 278 pp.

Song, J., and M. L. Banner, 2002: On the determining the onset and strength of breaking for deep water waves. Part I: Unforced irrotational wave groups. *J. Phys. Oceanogr.,* **32,** 2541–2558.

——, and ——, 2004: Influence of mean water depth and a subsurface sand bar on the onset and strength of wave breaking. *J. Phys. Oceanogr.,* **34,** 950–960.

Srokosz, M. A., 1986: On the probability of breaking in deep water. *J. Phys. Oceanogr.,* **16,** 382–385.

Toffoli, A., A. Babanin, M. Onorato, and T. Waseda, 2010: The maximum steepness of oceanic waves: Field and laboratory experiments. *Geophys. Res. Lett.,* **37,** L05603, doi:10.1029/2009GL041771.

Tolman, H. L., 2008: A mosaic approach to wind wave modeling. *Ocean Modell.,* **25,** 35–47.

Tulin, M. P., and M. Landrini, 2001: Breaking waves in the ocean and around ships. *Proc. 23rd Symp. of Naval Hydrodynamics,* Val de Reuil, France, Office of Naval Research, 713–745.

Waseda, T., T. Kinoshita, and H. Tamura, 2009: Evolution of a random directional wave and freak wave occurrence. *J. Phys. Oceanogr.,* **39,** 621–639.

Xu, D., P. A. Hwang, and J. Wu, 1986: Breaking of wind-generated waves. *J. Phys. Oceanogr.,* **16,** 2172–2178.

Young, I. R., and A. V. Babanin, 2006: Spectral distribution of energy dissipation of wind-generated waves due to dominant wave breaking. *J. Phys. Oceanogr.,* **36,** 376–394.

Yuan, Y., C. C. Tung, and N. E. Huang, 1986: Statistical characteristics of breaking waves. *Wave Dynamics and Radio Probing of the Ocean Surface,* O. M. Phillips and K. Hasselmann, Eds., Plenum Press, 265–272.

Zakharov, V. E., A. I. Dyachenko, and A. O. Prokofiev, 2006: Freak waves as nonlinear stage of Stokes wave modulation instability. *Eur. J. Mech.,* **25B,** 677–692.

Zaslavskii, G. M., and E. A. Sharkov, 1987: Fractal features in breaking wave areas on sea surface. *Dokl. Akad. Nauk SSSR,* **294,** 1362–1366.